IN VIVO BLOOD OXYGENATION LEVEL MEASUREMENTS USING PHOTOACOUSTIC MICROSCOPY

A Thesis

by

MATHANGI SIVARAMAKRISHNAN

Submitted to the Office of Graduate Studies of
Texas A&M University
in partial fulfillment of the requirements for the degree of

MASTER OF SCIENCE

May 2006

Major Subject: Biomedical Engineering

IN VIVO BLOOD OXYGENATION LEVEL MEASUREMENTS USING PHOTOACOUSTIC MICROSCOPY

A Thesis

by

MATHANGI SIVARAMAKRISHNAN

Submitted to the Office of Graduate Studies of
Texas A&M University
in partial fulfillment of the requirements for the degree of

MASTER OF SCIENCE

Approved by:

Chair of Committee,	Lihong V. Wang
Committee Members,	Alvin T. Yeh
	George Stoica
Head of Department	Gerard L. Coté

May 2006

Major Subject: Biomedical Engineering

ABSTRACT

In vivo Blood Oxygenation Level Measurements Using

Photoacoustic Microscopy. (May 2006)

Mathangi Sivaramakrishnan, B.E.(Hons.), Birla Institute of Technology and Science;

M.Sc.(Hons.), Birla Institute of Technology and Science

Chair of Advisory Committee: Dr. Lihong V. Wang

We investigate the possibility of extracting accurate functional information such as local blood oxygenation level using multi-wavelength photoacoustic measurements. Photoacoustic microscope is utilized to acquire images of microvasculature in small-animal skin. Owing to endogenous optical contrast, optical spectral information obtained from spectral photoacoustic measurements are successfully inverted to yield oxygenation level in blood. Analysis of error propagation from photoacoustic measurements to inverted quantities showed minimum inversion error in the optical wavelength region of 570-600 nm. To obtain accurate and vessel size independent blood oxygenation measurements, transducers with central frequency of more than 25 MHz are needed for the optical region of 570-600 nm used in this study. The effect of transducer focal position on accuracy of blood oxygenation level quantification was found to be negligible. To obtain accurate measurements *in vivo*, one needs to compensate for factors such as spectral dependent optical attenuation.

To my parents, grandparents and sisters.

ACKNOWLEDGMENTS

I would like to express my gratitude to my thesis advisor Dr.Lihong Wang for providing me with an opportunity to work in the Optical Imaging Laboratory under his esteemed guidance. The past few years spent at this lab has been a great learning experience.

I would like to express my thanks to Dr.George Stoica, who helped me understand and draw inferences from results of animal experiments. I would like to extend my thanks to Dr.Alvin Yeh who encouraged me throughout the project.

I am greatly indebted to Dr.Konstantin Maslov for guiding me at every step of my thesis and for being patient with me. Without his encouragement, guidance and support, completion of this thesis would not have been possible.

My thanks are due to all members of the Optical Imaging Laboratory for the support extended to me during my stay in the lab.

Finally, I owe my thanks to my parents, sisters and grandparents, for always believing in me and for their love and support throughout.

TABLE OF CONTENTS

CHAPTER Page

LIST OF FIGURES

CHAPTER I

INTRODUCTION

1. Research Objectives

This research project is aimed at using Photoacoustic Microscopy (PAM) for *in vivo* quantification of blood oxygenation level. Blood oxygenation level is an important physiological parameter that reflects on the overall efficiency of cardio-respiratory function and can yield localized information about tissue oxygenation. Pulse oximetry based on near infrared spectroscopy (NIRS) is currently the most widely used technique for this purpose in clinical settings. Several other single point measurement techniques like transcutaneous oxygen tension measurements and functional imaging modalities such as Blood Oxygenation Level Dependent functional Magnetic Resonance Imaging (BOLD fMRI), Electron Paramagnetic Resonance Imaging (EPRI), Positron Emission Tomography (PET), and Single Photon Emission Computed Tomography (SPECT) have capabilities to provide blood oxygenation information. There are several disadvantages attributed to each of the aforementioned imaging techniques, the common being the need for contrast agents. Photoacoustic imaging utilizes the endogenous blood contrast to quantify blood oxygenation level by exploiting the difference in the absorption spectra between oxygenated and deoxygenated hemoglobin, thus providing a spatial map of the blood oxygenation level. After demonstrating the use of Photoacoustic imaging to quantify blood oxygenation level, this study aims at optimizing the experimental parameters for improving the accuracy of such functional measurements. The project

---

This thesis follows the style and format of Applied Optics.

uses the dark-field confocal Photoacoustic Microscopy system developed in the Optical Imaging Laboratory, Texas A&M University.

2. Importance of Oxygenation Measurements: Motivation

Blood oxygenation saturation is defined as the oxygen content expressed as a percentage of the oxygen capacity. From the definition, SO_2 can be expressed as the ratio of concentration of oxygenated hemoglobin to the total hemoglobin concentration (sum of oxygenated and deoxygenated hemoglobin) in blood. The following describes a few biomedical applications of non-invasive oxygenation measurements.

Pulmonary and tissue oxygenation

Blood oxygenation level in general is reflective of the efficiency of cardio-pulmonary function while oxygenation level in the circulatory system provides an estimate of tissue oxygenation. While pulse oximetry measures arterial blood saturation and is indicative of only the pulmonary oxygenation, with the knowledge of localized arterial and venous oxygenation levels, tissue oxygenation level can be extracted. Indirect calorimetry is currently the gold standard to measure pulmonary oxygenation level. Oxygenation profiles enable the understanding of the patient's progress and response to treatment.[1]

Tumor hypoxia and treatment options

Non-invasive measurement of oxygen concentration in tissue has several implications in biomedical research. Hypoxia, a condition that often exists in tumors, has been found to be a barrier to effective treatment of cancer with radiation or

chemotherapy.[2,3] Measurements using oxygen electrodes have demonstrated that some human tumors contain hypoxic regions and the extent of hypoxia can have a profound effect on the tumor response to treatment. Studies have also indicated that the presence of hypoxia is an indicator of tumor aggressiveness.[4,5] All of the findings allude to the fact that apriori knowledge of pO_2 levels in tumors is important for selecting appropriate and effective treatment options. The ability to perform multiple timeline measurements to assess the impact of tumor hypoxia on treatment response and evaluation of new agents non-invasively would be extremely useful in the field of oncology and related research.

Cerebral blood oxygenation

Brain is highly responsive to changes in blood oxygenation level and blood flow and hence mapping to total hemoglobin (HbT) and hemoglobin oxygen saturation is of importance in neurophysiology, neuropathology and neurotherapy. For example, visualizing functional parameters of brain cancers and traumatic brain injuries, monitoring ischemia and shock, and studying neuronal activities are of interest. Despite decades of efforts, no technique has been developed until now that is clinically feasible for high-resolution, accurate, continuous and non-invasive imaging of HbT and SO_2 in organs, such as brain. Recently, circular scanning Photoacoustic Tomography has been used to localize and quantify the hemodynamic response to neural activities such as whisker stimulation in small animals with high spatial resolution of 60 μm. In addition, the ability of PAT to image global response to different inhalation conditions leading to normoxia, hyperoxia and hypoxia statuses has been demonstrated.[6]

Skin oxygenation measurements

Oxygenation measurements of blood in skin are critical in cancer research, dermatology and plastic surgery. Research has revealed that oxygenation level is an important factor for healing of burns,[7] wounds[8] and affects effectiveness of chemo and radio therapy for cancer.[9] The ability of burned skin to regenerate depends on the extent and depth of injury. Severely burned areas of skin have very limited blood supply, resulting in ischemia and eventually necrosis. The damage of blood vessels in the injured area alters the hemodynamics and a measure of this change might provide an estimate of the extent of injury. Wound healing involves a cascade of processes in order to carry out repair. One of the critical parameters for wound healing is oxygen delivery.[10] Hemoglobin, present in two distinct states of oxygenation, can provide an estimate of the oxygen supply and efficiency of oxygen utilization by tissue.

Peripheral vascular disease

Measuring local hypoxia is critical for the management of peripheral vascular disease, which commonly occurs in patients with conditions such as diabetes mellitus, hypertension etc.[11,12] Hypoxia could lead to limb dysfunction and eventually amputation of limb, depending on the severity of the condition. Non-invasive evaluation of tissue oxygenation would provide information about tissue viability and hence predict the extent of surgery or amputation required.

Myopathies and exercise physiology

With the advent of NIRS, the possibility of non-invasively monitoring the hemodynamics in brain and muscle tissue has been explored in the past years.

Information on muscle tissue oxygenation can serve to understand the mechanisms behind exercise physiology in detail and also pathologies related to myopathies.[11,13]

Calciphylaxis

Calciphylaxis is characterized by formation of calcifications in subcutaneous arterioles and venules.[14] This vasculopathy causes ischemia of the skin and subcutaneous tissues that leads to tissue necrosis in most cases. Studies have revealed that patients with renal failure are more frequently affected by Calciphylaxis and the occurrence is associated with very high mortality rates. Calcification of tissues such as tongue, mesenteric vasculature and heart valves has been reported. Histological characteristics of calciphylaxis include small-vessel calcifications of skin, subcutaneous tissue, and visceral organs. Recent reports indicate that the prevalence of the disease may be about 4% in dialysis patients. In most cases, the disease is diagnosed after extensive micro-vascular calcification has led to irreversible tissue injury, leading to eruption of skin lesions. Obviously, non-invasive detection of local hypoxia leading to diagnosis of the disease while still in its early stages would prove to be highly valuable. PAM has the potential for early diagnosis of the disease, assessment of severity of disease and monitoring disease progression.

Also, regional disturbances in the balance between oxygen delivery and utilization have important implications in the survival of transplanted tissue and tissue regeneration following micro-vascular surgery.[15]

3. Currently Available Techniques for Blood Oxygenation Measurements

Oxygen electrode measurements

Measurement of arterial oxygen tension using transcutaneous oxygen electrode is commonly used for monitoring health of infants. The device consists of a polarographic oxygen electrode that is in contact with skin through a thin membrane. The skin below the electrode is heated and leads to vasodilation and hence increased blood flow. Thus the amount of oxygen consumed by the skin is small as compared to the amount of oxygen available through hyperfusion. Oxygen that diffuses from the top most dilated capillaries is detected by the electrodes. The method has been successfully used in both infants and adults to monitor transcutaneous oxygen tension that correlates with arterial oxygen tension.[16] The caveat is that the success of the method critically depends upon the skin being heated sufficiently to allow diffusion of oxygen but not cause damage to the skin.

Near Infrared Spectroscopy

Near Infrared Spectroscopy (NIRS) offers the capability for continuous, non-invasive monitoring of cerebral metabolism.[17] Using NIRS, both blood oxygenation level and tissue oxygenation level can be obtained. The difference in absorption spectra of oxygenated (HbO_2) and deoxygenated hemoglobin (Hb) is exploited to yield oxygenation level information. This method consists of using Light Emitting Diodes (LEDs) as light sources to deliver light of known intensity and wavelength through tissue of interest and measuring the light intensity exiting the tissues, using photodiode or photomultiplier tube. Modified Beer-Lambert law, which allows for differential

pathlength compensation due to high scattering of light in biological tissue, is used to invert for the quantities of interest like concentration of the two dominant hemoglobin species, HbO_2 and Hb. NIRS can be used on any part of the body, although cerebral oxygenation has been explored in detail. The inter subject variability of differential pathlength factor (DPF) is one of the major problems in NIRS. In case of infants due to small size of the head, transmittance measurements can be used while in adults, diffuse reflectance measurements are utilized.

Although deep light penetration and ease of measurements make this a preferred technique, it lacks spatial resolution and hence cannot provide a spatial map of the oxygenation level. Such information would be invaluable in assessing tumor hypoxia which is a critical parameter for treatment planning.[18]

Pulse oximetry

Currently, pulse oximetry is the technique that is widely used in clinical settings.[19] The principle is based on NIRS, but the measurements are time-gated to separate the pulsatile component to yield arterial blood saturation only. Since the ratio of concentrations of HbO_2 and Hb is the factor being quantified, the effect of DBF is nullified. The disadvantage of the technique is that it yields single point measurements of arterial blood saturation only and lacks spatial resolution. Albeit, this is most preferred and extensively used clinically due to the portability and ease of measurements.

Positron Emission Tomography (PET)

Emission Tomography is technique in nuclear medicine that visualizes the distribution of radionuclide introduced into the patient's body prior to imaging. This

method is based on detecting the annihilation radiation that is generated when positrons are absorbed in matter. The reconstructed image provides an accurate and quantitative representation of the spatial distribution of the radionuclide in the images transverse section of the body.

It is possible to image blood volume and blood flow using this modality. By using both labeled O_2 and CO_2, local oxygen metabolism can be studied. A combination of PET and MRI can utilize the changes in blood flow associated with activities associated with brain and hence can be used in neuroscience research.

Single Photon Emission Computed Tomography (SPECT)

SPECT is a diagnostic imaging modality that yields tomographic slices of internally distributed radiotracer. It is commonly used for diagnosing coronary artery disease and tumor detection. Projection views of the distribution of the injected tracer collected by scintillation cameras that are mounted to rotate around the patient lying horizontally are mathematically reconstructed to obtain the slices. In this modality, gamma rays are detected as individual events. The term “single photon” is used to distinguish SPECT from PET, which relies on coincidence imaging.

Diagnostic information can be obtained using this imaging technique by choice of appropriate tracer. For example, tumor detection is possible by using radio-pharmaceuticals that have affinity for malignant tissue. In these scans, abnormal areas are characterized by an increased uptake of the tracer. Usually, the tracer is systemically introduced into the body by intravenous injection and is carried throughout the body by blood circulation where it localizes in tissues and organs. This method allows regional

and quantitative evaluation of blood flow.[20] The most common diagnostic applications for SPECT include myocardial perfusion imaging, tumor scanning, brain perfusion for evaluating stroke and dementia, renal function and evaluation of trauma. As in case of PET, by introducing tracers to label both O_2 and CO_2, information on local oxygen metabolism can be obtained.

The widespread distribution of the radioactive tracer in the body has other implications, the most important being radiation dose. The quality of SPECT images is limited by the restriction on the amount of radioactive tracer that can be administered to the patient. Although these modalities can offer real-time information during scan, they are expensive, time consuming, not suitable for bed-side monitoring and need the use of contrast agents.

Blood Oxygenation Level Dependent (BOLD) MRI

BOLD MR imaging—the blood oxygen level-dependent (BOLD) contrast is obtained by accentuating the susceptibility effect of deoxyhemoglobin (dHb) in the venous blood with gradient-echo techniques. It was discovered that contrast of the obtained image reflected the blood oxygen level. As it is now known, it is due to the field inhomogeneities induced by the endogenous MRI contrast agent dHb. In the simplest model, these relaxation rates change linearly with deoxyhemoglobin concentration, which therefore acts as an endogenous contrast agent for blood oxygenation.

BOLD MRI is a non-invasive technique that can monitor real-time changes of oxygenation level with high spatial resolution. Changes in vascular development, tumor

hypoxia, tumor response to treatment, maturation and functional state of tumor can be studied. BOLD MRI is a non-quantitative method for monitoring pO_2. BOLD MRI can measure changes in blood oxygenation as opposed to static quantification. Inferences from measurements may be complicated by the fact the technique cannot differentiate the contrast of blood oxygenation level from blood flow.

Electron Paramagnetic Resonance Imaging (EPRI)

EPRI probes species with unpaired electrons, such as free radicals and transition metal complexes. Similar in MRI, spatial images are obtained by application of magnetic gradient fields. Like protons, the spin-spin relaxation time of electrons is influenced by molecular oxygen, which is paramagnetic; hence, oxygen can be used as an endogenous contrast agent to an exogenous paramagnetic spin probe suitable for in vivo imaging applications.

Since the naturally occurring paramagnetic species in the body are below the detection limit, contrast agents are required to conduct the procedure. The effect of contrast agents used for EPRI has been studied in detail and it is claimed that the toxicity of the probes is minimal.[21] The resonator design is critical as the sample must occupy the whole volume and must provide access to the sample for injection of anesthesia and contrast agents. It is possible to extract oxygen concentration in tissue on a voxel-by-voxel basis. This method has important implications in the study of tumor hypoxia, tissue heterogeneity with respect to oxygen and redox status, and vascular deficiencies in vivo. This modality shows promise in spatially resolving hypoxic regions and may

represent a noninvasive approach to estimate oxygen status differences in organs or any other regions of interest.

As described above, various techniques and imaging modalities exist that allow quantification of blood oxygenation level *in vivo*. Still, there is a growing need for a new modality that obviates the need for external contrast agents, provides a spatial map of oxygenation level and enables accurate quantification of the same.

4. Photoacoustic Imaging for Blood Oxygenation Measurements

Photoacoustic imaging is a hybrid non-invasive modality that yields images of high optical contrast and ultrasonic resolution. Short laser pulses are used to generate ultrasonic waves in biological tissues. The ultrasonic waves thus generated provide information about the absorption heterogeneity in tissues. Since blood is one of the main absorbers in biological tissue, vascular structure can be imaged. Similar to NIRS, by employing multiple wavelengths, it is possible to extract blood oxygenation level information using Photoacoustics. By utilizing the endogenous blood-tissue contrast, the spatial map of subcutaneous vasculature has been imaged with a resolution of 100μm[22,23] and functional information such as blood oxygenation level and total hemoglobin has been measured locally in rat brain cortex using circular scanning photoacoustic tomography.[6]

Since biological tissue is highly scattering, pure optical imaging techniques like diffuse optical tomography, fluorescence imaging or other microscopy, lack spatial resolution beyond the skin. The photoacoustic imaging technique, with merits of both

optics and ultrasound, is a powerful tool for visualizing biological tissues with satisfactory sensitivity and spatial resolution. Also, since this method utilizes the endogenous blood contrast, it eliminates the need for using potentially hazardous contrast agents as in case of EPRI, PET and SPECT. This also means that multiple timeline study is possible.

CHAPTER II

PHOTOACOUSTIC IMAGING

Imaging science has advanced over the decades and gained importance especially in the field of diagnosis. Because in most cases the location and extent of a disease is unknown, the first objective is an efficient means of searching throughout the body to determine its location. Imaging is an extremely efficient process for accomplishing this aim, because data are presented in pictorial form to the most efficient human sensory system for search, identification, and interpretation of the visual system. Recognition depends upon the type of information in the image, both in terms of interpreting what it means and how sensitive it is to identifying the presence of disease.

1. Basic Principle of Photoacoustic Imaging

Photoacoustic imaging (also known as opto-acoustic imaging or thermo-acoustic imaging) relies on the absorption of electromagnetic energy, such as light, and subsequent emission of acoustic waves (sound). Specifically, through the process of thermo-elastic expansion, broadband acoustic waves are generated through the irradiated volume. Under irradiation conditions of temporal stress confinement, the acoustic profiles generated can be utilized to reconstruct an image of the test sample. The pressure p(r, t) at position r and time t in an acoustically homogenous medium obeys the following equation:

$$\left(\nabla^2 - \frac{1}{c^2}\frac{\partial^2}{\partial t^2}\right) p(r,t) = -\frac{\beta}{C_p}\frac{\partial H(r,t)}{\partial t}, \tag{1}$$

where p is the acoustic pressure, c is the speed of sound, β is the isobaric volume expansion coefficient, C_p is the heat capacity per unit mass, t is time, and H is the heat deposited in the medium per unit volume and time.

Stress confinement criterion

When the width of the incident laser pulse is shorter than the transit time of the generated ultrasonic waves through the medium, temporal stress confinement criterion is said to be satisfied. Hence, $\tau_L << d/c$, where τ_L is the laser pulse duration, d is the optical penetration depth and c is the acoustic velocity, defines the stress confinement criterion. When the condition holds, the initial pressure distribution is directly proportional to the deposited energy density. For our experiments employing visible wavelengths, the optical pathlength is about 3 mm ($1/\mu_a$; μ_a for blood $\approx$ 290 cm^{-1}) and correspondingly, acoustic transit time is 2 μs which is much greater than 6.5 ns, the employed laser pulse width.

The PA pressure generated is directly proportional to the localized absorption in the imaged voxel. To map the heterogeneity of absorption in the tissue, focused ultrasonic transducers can be used to localize the photoacoustic sources in linear or sector scans and then construct the images directly from the data as is often done in pulse-echo ultrasonography.

When laser pulses at second harmonic wavelength of 532 nm from Nd:YAG laser are employed, the optical absorption of whole blood is much stronger than that of surrounding tissue. The absorption coefficient of human blood at this wavelength is nearly 200 cm^{-1}, which is almost 10 times higher than that of epidermis and nearly 500

times higher than that of dermis. Hence blood generates strong photoacoustic signals and manifests high image contrast, causing the vasculature in organs to stand out prominently in photoacoustic images. Besides optical absorption, the thermal and elastic properties of the tissues also affect the strength of photoacoustic signals. Therefore physical changes, such as density in a tissue, can be reflected in photoacoustic images.

Photoacoustic imaging comprises the following:

1. **Tissue is irradiated with a pulsed laser light at a specific wavelength.** Short laser pulses (5-10 ns long) are used – longer pulses do not satisfy the stress confinement criteria and hence conversion efficiency of absorbed energy to heat is reduced.

2. **Generation of ultrasound.** Absorbed optical energy is converted to thermal energy, followed by thermal expansion of tissue and generation of ultrasound (pressure) pulse. The temperature rise is estimated to be <100 mK. The contrast in Photoacoustic imaging is primarily determined by optical contrast between different types of tissues.

3. **The generated ultrasound signal is recorded using ultrasound transducer and is used to form an image.** The received ultrasound signal contains information about both position (time of flight) and strength of the optical absorber (amplitude of the signal).

The contrast mechanism in photoacoustic imaging, therefore, offers the prospect of identifying both anatomical features such as vasculature and functional parameters like blood oxygenation level and total hemoglobin in blood.

2. Dark-Field Confocal Photoacoustic Microscopy

A dark-field reflection-mode photoacoustic microscopy (PAM) system was developed in the Optical Imaging Laboratory, Texas A&M University. High resolution images (~60 μm) of rat cerebral vasculature have been obtained using circular scanning photoacoustic computed tomography.[6] Circular scanning mechanism works best for elevated objects such as brain or breast. Planar reflection-mode techniques do not suffer from shape constraints on the sample, but may suffer from strong photoacoustic signals from optical absorbers near the surface, which can overshadow the much weaker photoacoustic signals from deeper structures of interest. To overcome this problem, dark-field illumination system has been implemented. Since biological tissue is highly scattering, image resolution beyond one transport mean free path (~1 mm) is determined by ultrasound detection parameters. For high ultrasonic resolution, the detection transducer must have wide bandwidth and high numerical aperture. Due to linear ultrasonic attenuation with increasing detection frequency, (0.7 – 3 dB/cm/MHz for human skin), there has to be a trade-off between increasing the detection frequency of ultrasound and imaging depth. Therefore, large numerical aperture is necessary for improving the resolution. The optical focal region overlaps with the focal spot of ultrasonic detection, hence forming a confocal configuration of illumination and detection systems.[22,23]

3. System Details

The PAM system consists of a Q-switched pulsed Nd:YAG laser (Brilliant B, Bigsky) providing laser pulses at 532 nm (6.5 ns pulse width; 10 Hz pulse repetition rate) that acts as the pumping laser for tunable dye laser (ND6000, Continuum). The irradiation pulses are incident on the sample via a coaxially coupled fiber optic cable, expanded by a conical lens and then focused through an optical condenser with an NA of 1.1. The pulse energy is attenuated about a thousand fold and the laser fluence incident on the sample surface is estimated to be 3 mJ/cm^2, which is well within the maximum permissible exposure set by ANSI standards. A spherically focused ultrasound transducer (Panametrics) with a center frequency of 50 MHz and nominal bandwidth of 70% is attached to a home-made concave lens and placed in a confocal arrangement with the optical illumination. A low-noise amplifier and digital oscilloscope (TDS 5034B, Tektronics) constitute the data acquisition system. A computer controlled three-dimensional mechanical scanner allows precise positioning of the illumination and the detection systems for raster scanning along the x-y plane with a set step size and hence enables 3D data collection. A schematic of the PAM system is shown in fig 1.

If a single focused transducer is employed, as in case of PAM system, to provide one-dimensional images along the ultrasound axis and by linearly scanning the transducer, a two-dimensional image can be obtained. For this imaging configuration, the image resolution is determined by focal parameters and the bandwidth of the ultrasonic detection system.

Multi-wavelength PA measurements need to be acquired for extracting information on oxygenation level of blood. All spectral data for a single b-scan is collected before moving on to the next cross-section to minimize positioning errors.

With a 50 MHz, 0.44 NA transducer, the PAM system is capable of imaging skin vasculature up to 3 mm deep, with a lateral resolution of 40-120 μm *in vivo* depending on imaging depth and high axial resolution of 15 to 30 μm.[22,23] For other transducers used in this study (25MHz, 0.26NA and 10MHz, 0.26NA), resolution degrades with transducer central frequency and numerical aperture.

To correct for the instability in laser output, each A-Line data acquired was normalized by the incident laser pulse energy measured using a photodiode. The various peaks along the A-lines were identified and corresponding spectral values were used for pixel by pixel calculation of SO_2. Published values of molar extinction coefficients for HbO_2 and Hb were used for this purpose.[24]

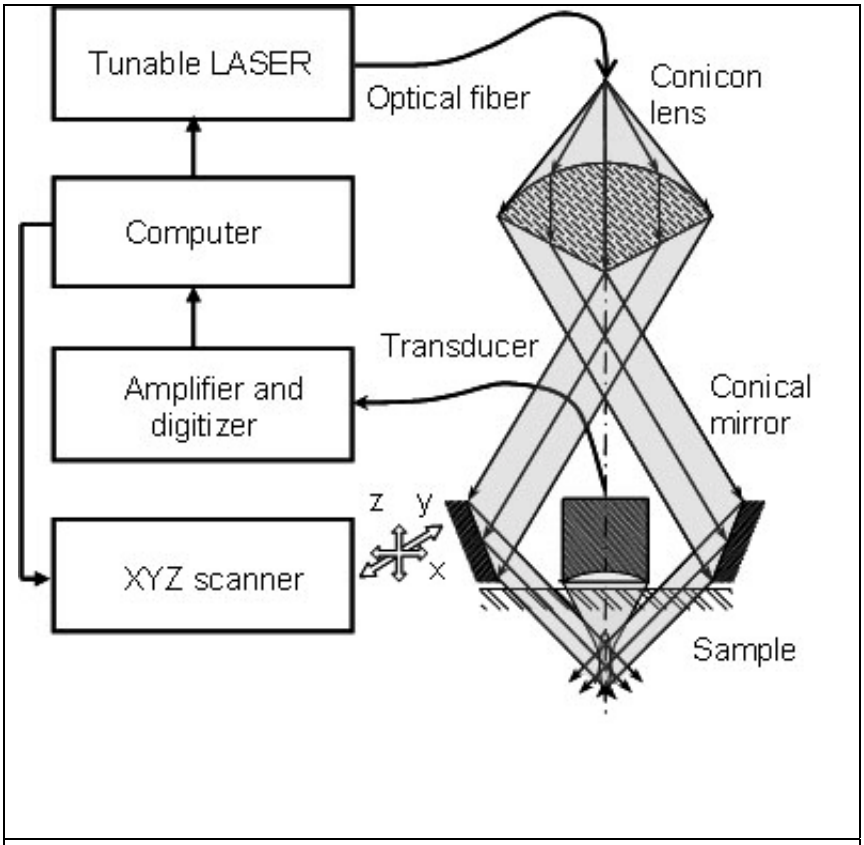

Fig. 1. Schematic of the PAM system

4. Oxygenation Measurements Using PA

As shown in fig 2, although melanosomes are strong absorbers in biological tissue, considering that their volume fraction in epidermis is low,[24] it can be assumed that blood is the dominant light absorber in the visible light regime. Hence, the total absorption coefficient at a given wavelength λ can be given by:

$$\mu(\lambda) = \mu_{HbO2}(\lambda) + \mu_{Hb}(\lambda) \tag{2}$$

where, $\mu_{HbO2}(\lambda)$ and $\mu_{Hb}(\lambda)$ are the absorption coefficients of oxygenated and deoxygenated hemoglobin respectively, the two main species of hemoglobin in the body.

Further, $\mu_{HbO2}(\lambda)$ can be given by $\varepsilon_{HbO2} \times [HbO_2]$, where ε_{HbO2} is the known molar absorption coefficient of HbO_2 and $[HbO_2]$ is the concentration of oxygenated hemoglobin (similarly for deoxy hemoglobin). Hence, (1) can be written as

$$\mu(\lambda) = \varepsilon_{HbO\,2}(\lambda)[HbO_2] + \varepsilon_{Hb}(\lambda)[Hb] \tag{3}$$

The PA signal is a function of the product of absorption coefficient and fluence rate. Assuming that PA signal is proportional to the optical absorption of a voxel, for any given wavelength λ_i, $\phi(\lambda_i) \propto \mu(\lambda_i) \Rightarrow \phi(\lambda_i) = \mathrm{K} \times \mu(\lambda_i)$ where K is some constant. From multi-wavelength measurements, a system of linear equations can be obtained, which can be written in the following matrix format.

$$\begin{bmatrix} \varepsilon_{HbO_2}(\lambda_1) & \varepsilon_{Hb}(\lambda_1) \\ \varepsilon_{HbO_2}(\lambda_2) & \varepsilon_{Hb}(\lambda_2) \\ . & . \\ . & . \\ . & . \\ \varepsilon_{HbO_2}(\lambda_n) & \varepsilon_{Hb}(\lambda_n) \end{bmatrix} \times \begin{bmatrix} [HbO_2] \\ [Hb] \end{bmatrix} = K \begin{bmatrix} \phi(\lambda_1) \\ \phi(\lambda_2) \\ . \\ . \\ . \\ \phi(\lambda_n) \end{bmatrix} \tag{4}$$

Solving the system of equations by method of least squares, blood oxygenation level can be obtained using the following:

$$\begin{bmatrix} [HbO_2] \\ [Hb] \end{bmatrix} = (M^T M)^{-1} M^T \Phi \; ; \; SO_2 = \frac{[HbO_2]}{[HbO_2] + [Hb]},$$

where $M = \begin{bmatrix} \varepsilon_{HbO_2}(\lambda_1) & \varepsilon_{Hb}(\lambda_1) \\ \varepsilon_{HbO_2}(\lambda_2) & \varepsilon_{Hb}(\lambda_2) \\ . & . \\ . & . \\ . & . \\ \varepsilon_{HbO_2}(\lambda_n) & \varepsilon_{Hb}(\lambda_n) \end{bmatrix}$ and $\Phi = \begin{bmatrix} \phi(\lambda_1) \\ \phi(\lambda_2) \\ . \\ . \\ . \\ \phi(\lambda_n) \end{bmatrix}$

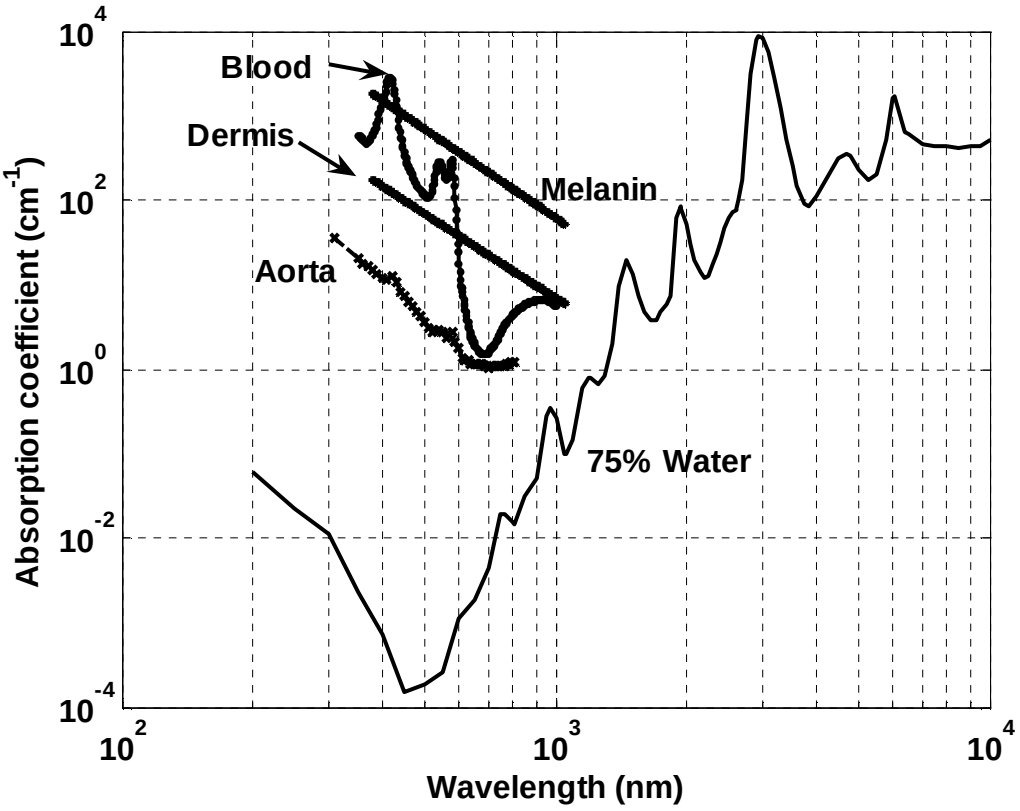

Fig. 2. Absorption spectra of primary absorbers in biological tissues. Note that blood is the primary absorber in the visible region given that the volume fraction of melanosomes is negligible.[24]

5. Advantages of Photoacoustic Imaging

Pure optical imaging techniques employ non-ionizing radiation and have advantages of high sensitivity and low cost and hence are advantageous for functional and diagnostic imaging. The main challenge faced by optical imaging techniques is the highly scattering property of biological tissues, which limits both resolution and depth of imaging. With the advent of several optical imaging modalities like Confocal Microscopy, Optical Coherence Tomography (OCT), satisfactory imaging resolution has been achieved. Since these techniques are based on the detection of ballistic photons, the imaging depth is limited to about a millimeter. On the other hand, Diffuse Optical Tomography (DOT) provides better imaging depth although resolution is degraded by scattering.

Since photoacoustic imaging is based on ultrasonic signal propagation and detection, the resolution comparable to that of pure ultrasound imaging while image contrast is based on optical absorption. Further, PA imaging is free of the speckle artifacts presented in OCT and ultrasonography, because photoacoustic waves travel only one way to reach the ultrasonic detector rather than two ways as in OCT and ultrasonography. Hence this modality combines advantages of pure optical and pure ultrasonic imaging, thus providing high contrast and high resolution images.

CHAPTER III

PRELIMINARY STUDIES

Proof of principle experiments on phantoms and blood samples were conducted with the objective of demonstrating the capability of the PAM system to perform functional measurements.

1. Phantom Studies

To demonstrate the capability of the PAM system to quantify the concentration of two absorbing components in a mixture, phantom studies were conducted using samples with different volumetric ratios of red and blue inks (Private Reserve Ink). The stock samples of red and blue inks were prepared by diluting the inks from the bottles 50 and 80 times respectively. Optical wavelengths of 578 – 596 nm in steps of 6 nm were employed and 50 MHz transducer was used for this study. The samples were injected into transparent tubes (TYGON S-54-HL, Norton Performance Plastics) of inner diameter 0.25 mm. The tubes were attached to a home-made plastic casing which was immersed in water for ultrasound coupling. Single point measurements were acquired and the signals were averaged ten times. Fig 3(a) shows the plot of concentration fractions inverted from photoacoustic measurements against the preset concentration fractions given by [Red]/([Red]+[Blue]) and they are found to match with less than 1% error.

2. *In vitro* Blood Studies

Bovine blood samples (with anticoagulant citrate dextrose solution) of different oxygenation levels were used as samples. Two stock samples were made by mixing the blood with pure oxygen and carbon-dioxide respectively.[25] Nine more samples of different oxygenation levels were made by mixing these two stock samples at different volumetric ratios. SO_2 values obtained from NIRS measurements on hemolyzed samples were used as "gold standard". Since blood is highly scattering, a part of each of the blood samples was hemolyzed using 0.5% saponin solution (10% v/v) and let sit for 30 minutes. The red blood cells get lysed in the process and precipitate. The liquid devoid of RBCs has much less scattering (negligible as compared to absorbance) and NIRS spectroscopic measurements in the wavelength range of 700-1000 nm were obtained in steps of 8 nm on these samples.[26] Transparent tubes of inner diameter 0.25 mm were used and the sample was allowed to flow through the tube at a constant rate of ~0.3 ml/hr to prevent sedimentation. Single point measurements were acquired and the A-Line signals were averaged 30 times. Published molar extinction values of bovine blood were used for the SO_2 calculations. Fig 3(b) shows plot of SO_2 data obtained from PAM measurements against the spectrophotometric results. The results agree with a systematic error of ~4%.

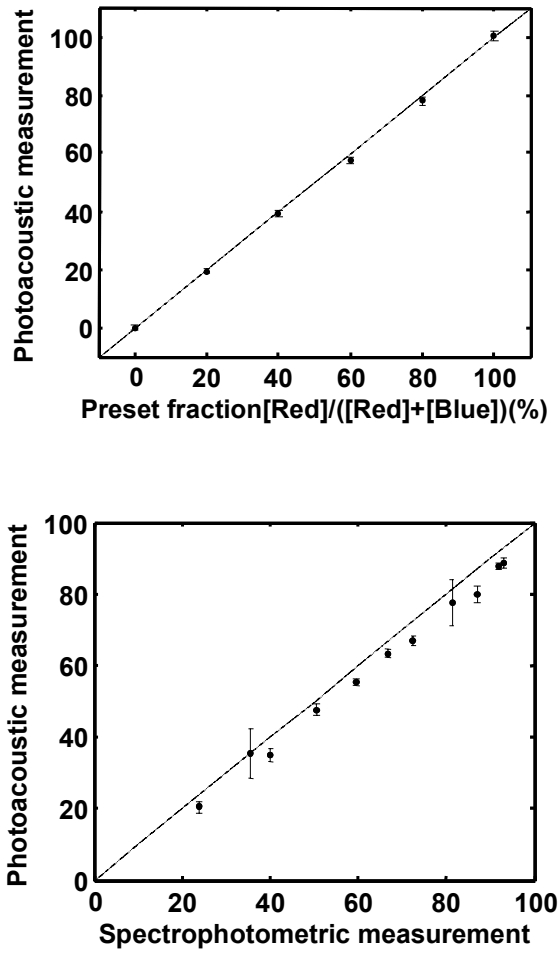

Fig. 3. Spectroscopic PA measurement of ink and blood samples *in vitro*.

(a) Photoacoustic measurement of fraction of the red dye in the mixture of two dyes, [Red]/([Red]+[Blue]), as a function of volumetric dye ratio. (b) Comparison of photoacoustic measurement and the spectrophotometric measurement of SO_2 in bovine blood samples *in vitro*.

3. PA Signal Saturation with Highly Absorbing Samples

Having demonstrated through phantom and blood studies, the capability of the PAM system for oxygenation measurements, phantom studies were done to show the occurrence of saturation with highly absorbing samples. Different concentrations of black ink (Private Reserve Ink) were used and PAM measurements were made on these samples with 50 MHz transducer at 590 nm. Fig (4) shows the plot of PA signal after compensation for laser instability against the preset concentration of the samples used. PA signal saturation was observed with increasing concentration of black ink (and hence increasing absorption).

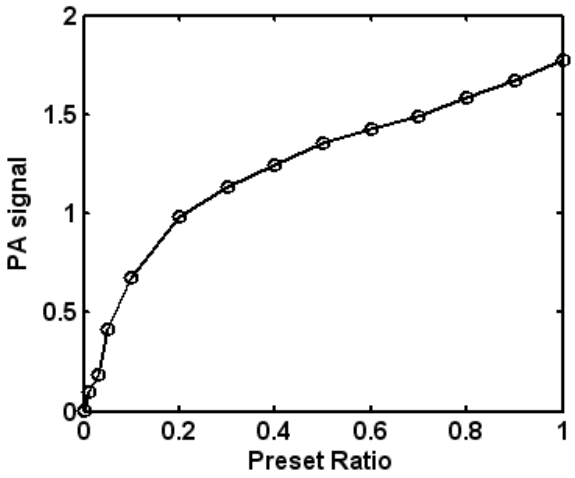

Fig. 4. PA signal saturation on highly absorbing black ink samples. Peak amplitude of photoacoustic signal from increasing concentrations of black ink samples showing PA signal saturation

CHAPTER IV

TECHNICAL CONSIDERATIONS FOR ACCURATE BLOOD OXYGENATION LEVEL MEASUREMENTS USING PHOTOACOUSTICS

1. Need for Optimization of Experimental Parameters

From the results of preliminary experiments, it is possible to quantify blood oxygenation level using multi-wavelength PA measurements. The choice of experimental parameters determines the accuracy of such measurements. Some of the parameters that affect the accuracy of measurements are the choice of optical illumination wavelengths, ultrasonic detection bandwidth, object size and shape and spectral dependence of optical fluence reaching the absorber.

PA signal is proportional to absorbed light energy, which at certain conditions is a linear function of μ_a. Since blood provides the contrast for PA imaging, to improve the signal to noise ratio and imaging resolution, visible light in the wavelength range of 570-600nm, where blood absorption is high, is chosen for measurements. In order for the system of linear equations to converge, the slopes of the spectra of the absorbing species have to be very different and this condition is satisfied in the chosen visible range. There are a few spectral regions where these conditions hold. Highest sensitivity and contrast is obtained in the 570-600 nm range. Blood has very high absorption in this region as compared to near infra-red and consequently, light penetration in blood vessel is limited in the visible regime. When light penetration is shorter than ultrasonic wavelength, signal saturation occurs because the entire incident light is absorbed. The PA signals

become absorption (or wavelength) independent and hence accuracy of SO_2 quantification is compromised. Hence for reasonable quantification of SO_2 in the chosen illumination regime, high frequency transducers are required. The choice of the transducer bandwidth is determined by the penetration depth of the illumination wavelengths and hence dependent on the absorption coefficient of the absorbing species.

In the chosen wavelength regime, for the maximum absorption, light penetration in blood is ~ 30 μm. To avoid signal saturation, assuming the best possible resolution for a transducer, this number translates an ultrasonic frequency of 50 MHz.

Owing to highly scattering property of biological tissues, the resolution of PA signals beyond one transport mean free path into biological tissue is primarily determined by ultrasonic detection parameters. The axial resolution is governed by Abbe-Rayleigh resolution criterion: $\xi = 0.66\frac{\lambda}{\sin(\theta)}$,

where λ is the acoustic wavelength and θ is the focusing transducer aperture angle. From the equation, it is evident that by improving the detection ultrasonic frequency, the resolution can be improved.

For a simple one dimensional model, which is a valid approximation when blood vessel radius is bigger then focal spot size, equation (1) has a simple solution in frequency domain:

$$|p(\omega)| = \frac{\beta}{2C_p} I\mu_a c \frac{h(\omega)}{\sqrt{\mu_a^2 + (\frac{\omega}{c})^2}}, \qquad (5)$$

where ω is ultrasonic frequency, I is optical fluence, μ_a optical absorption, and h(ω) is Fourier transform of laser pulse. As it is clear from equation (5), if optical absorption exceeds ultrasonic wavenumber, photoacoustic pressure becomes independent of optical absorption. On the other hand, if optical absorption is too small, pressure magnitude drops down inversely proportionally to ultrasonic frequency. Definitely, optimal choice of experimental parameters is necessary to achieve correct quantitative measurements from spectroscopic photoacoustic imaging.

2. Inversion of Tissue Parameters from Spectral PA Measurements

It is reasonable to state that PA signal from blood vessel, $A_k(p_\alpha)$, which can be, for example, peak-to-peak voltage or peak amplitude of Hilbert transfer of transducer voltage, is a unique function of tissue parameters, p_α, such as hemoglobin concentration, (HbR), and oxyhemoglobin concentration, (HbO_2), ultrasonic attenuation, vessel size and position, and illumination condition which itself is a function of tissue optical scattering and absorption. If PA signal can be theoretically calculated from known p_α at wavelengths λ_k, tissue parameters can be inverted by minimizing difference between experimentally measured, A_k^e, and calculated PA signals, in least square sense. Mathematically, true tissue parameters are those which render following error function minimal:

$$\frac{\partial E}{\partial p_\alpha} = \frac{1}{N}\frac{\partial}{\partial p_\alpha}\sum_{k=1}^{n}\left(A_k^e - A(p_\alpha(\lambda_k))\right)^2 = 0, \qquad (6)$$

Near correct solution linear expansion can be used to express change of measured PA signal with change of tissue parameters:

$$\Delta A_k = \frac{p_j}{A_k}\frac{\partial A_k}{\partial p_j}\Delta p_\alpha = S_{k\alpha}\Delta p_\alpha \ , \tag{7}$$

where S_{jk} are sensitivities of the PA signal at wavelength *k* to parameter *j*. Eq. (6) can be inverted as $\Delta p_\alpha = (S_{\beta k}S_{k\alpha})^{-1}S_{\beta l}\Delta A_l^e$. (8)

3. Error Propagation in Inversion for SO_2 Values:

Interesting quantities in research are often derived from the basic measurements by calculations involving transformations, inversions etc. It is possible to understand the uncertainty characteristics of the derived quantities from those of the measured quantities. In the context of extracting quantitative information from measured PA signals, such analysis would give us an insight into the propagation of random perturbations (such as additive electronic noise) in PA measurements into errors in inverted quantities of oxygenation level and total hemoglobin through the matrix inversion procedure. Understanding this propagation is important, for example, to help us select the optimal choice of optical wavelengths for the quantifying the chromophores of interest.

The PA pressure generated is proportional to the local optical absorption and can be written in terms of the molar extinction coefficients and concentrations of the absorbing species.

For spectral PA measurements, $PA_{\lambda_i} = K(C_{HbO_2}\times\varepsilon_{HbO_2,\lambda_i} + C_{Hb}\times\varepsilon_{Hb,\lambda_i})$, where PA_{λ_i} is the PA signal amplitude at wavelength λ_i , C_{HbO_2} is the concentration of

oxyhemoglobin in blood, C_{Hb} is the deoxyhemoglobin concentration in blood and K is the proportionality constant between incident light energy density and PA signal generated. Rewriting the above equation in terms of the inverted quantities:

$$SO_2 = \frac{C_{HbO_2}}{C_{HbO_2} + C_{Hb}}; C_{HbT} = C_{HbO_2} + C_{Hb}; C_{HbO_2} = SO_2 \times C_{HbT}; C_{Hb} = (1 - SO_2) \times C_{HbT}$$

$$PA_{\lambda_i} = K(SO_2 \times C_{HbT} \times \varepsilon_{HbO_2,\lambda_i} + (1 - SO_2) \times C_{HbT} \times \varepsilon_{Hb,\lambda_i}) \quad (9)$$

Using chain rule, the error in inverted quantities can be written in terms of perturbations in PA measurements as:

$$\delta PA_{\lambda_i} = \frac{\partial PA_{\lambda_i}}{\partial SO_2} \times \delta SO_2 + \frac{\partial PA_{\lambda_i}}{\partial C_{HbT}} \times \delta C_{HbT} \quad (10)$$

Writing (4) in matrix format:

$$\begin{bmatrix} \delta PA_{\lambda_1} \\ \delta PA_{\lambda_{21}} \\ . \\ . \\ . \\ \delta PA_{\lambda_N} \end{bmatrix} = \begin{bmatrix} \frac{\partial PA_{\lambda_1}}{\partial SO_2} & \frac{\partial PA_{\lambda_1}}{\partial C_{HbT}} \\ \frac{\partial PA_{\lambda_2}}{\partial SO_2} & \frac{\partial PA_{\lambda_2}}{\partial C_{HbT}} \\ . & . \\ . & . \\ . & . \\ \frac{\partial PA_{\lambda_N}}{\partial SO_2} & \frac{\partial PA_{\lambda_N}}{\partial C_{HbT}} \end{bmatrix} \begin{bmatrix} \delta SO_2 \\ \delta C_{HbT} \end{bmatrix} \Rightarrow \hat{X} = \underbrace{(A^T A)^{-1} A^T}_{M} P \quad (6)$$

$$\underbrace{\quad}_{P} \quad \underbrace{\quad}_{A} \quad \underbrace{\quad}_{X}$$

The sensitivities of the PA signal to each of the change in the derived quantities constitute the sensitivity matrix. The sensitivities can be computed from

$$\frac{\partial PA_{\lambda_i}}{\partial SO_2} = C_{HbT} \times (\varepsilon_{HbO_2,\lambda_i} - \varepsilon_{Hb,\lambda_i}); \frac{\partial PA_{\lambda_i}}{\partial C_{HbT}} = SO_2 \times (\varepsilon_{HbO_2,\lambda_i}) + (1 - SO_2) \times \varepsilon_{Hb,\lambda_i} \quad (11)$$

The errors in PA signal can be fairly assumed to be Gaussian with zero mean. Let each measured PA signal have a wavelength independent additive error with variance σ^2. The variance for a measurement set can be expressed, in matrix form, as the covariance matrix: $\text{cov}(\hat{X}) = \text{cov}(MP) = <(MP\ (MP)^T> = < MPP^TM^T > = M<PP^T>M^T = M\sigma^2IM^T = \sigma^2MM^T = \sigma^2(A^TA)^{-1}$

Assuming that measurement error is a wavelength independent additive error with variance $\sigma_A^2 = \hat{E}$, where $\hat{E}$ is the residual value of E at convergence, (8) can be used to estimate covariance of inverted parameters: $\Delta p_\alpha (S_{\beta k} S_{k\alpha}) \Delta p_\beta \approx \hat{E}$. (12)

Consequently, the variance bounds for a single parameter Δp_Z are proportional to residual error $\sqrt{\hat{E}}$ multiplied by the error propagation factor (EPF)[27] for Δp_Z :

$$\Delta p_Z \approx \pm \left[C_{ZZ} - C_{Z\xi} C_{\xi\zeta}^{-1} C_{\zeta Z} \right]^{-1/2} \sqrt{\hat{E}}\ , \tag{13}$$

where $C_{\beta\alpha} = S_{\beta k} S_{k\alpha}$, $\xi, \zeta = 1, 2, ..., Z-1, Z+1, Z+2, ..., \eta$ and η is the number of independent parameters.

The PA signal is calculated from the published spectra of molar extinction for HbR and HbO_2, that is, $\varepsilon_{a,HbR}(\lambda)$ and $\varepsilon_{a,HbO_2}(\lambda)$, respectively, using a linear regression technique[28] that assumes that the PA signal is linearly proportional to the optical absorption of hemoglobin and the optical fluence at the blood vessel surface as already shown by equation (4):

$$\begin{bmatrix} A(\lambda_1) \\ A(\lambda_2) \\ . \\ . \\ . \\ A(\lambda_n) \end{bmatrix} = K \begin{bmatrix} \varepsilon_{HbO_2}(\lambda_1) & \varepsilon_{HbR}(\lambda_1) \\ \varepsilon_{HbO_2}(\lambda_2) & \varepsilon_{HbR}(\lambda_2) \\ . & . \\ . & . \\ . & . \\ \varepsilon_{HbO_2}(\lambda_n) & \varepsilon_{HbR}(\lambda_n) \end{bmatrix} \times \begin{bmatrix} [HbO_2] \\ [HbR] \end{bmatrix},$$

where, K is the unknown coefficient of proportionality between the incident light intensity and the PA signal magnitude, believed to be wavelength independent. Equation (11) can be inverted for hemoglobin concentrations [HbR] and [HbO_2], and $SO_2 = [HbO_2]/([HbO_2]+[HbR])$ can be calculated by matrix inversion as a function of the known Hb spectra and the measured PA amplitudes.

Sensitivity matrix A can be calculated from (11) for a chosen SO_2 level and the normalized variance in the inverted quantities is plotted as a function of wavelength as shown in fig 5(b). It is interesting to note that the variance in the PA measurements only acts as a scaling factor while the variance inverted quantities depend on the molar extinction coefficient of the absorbing species.

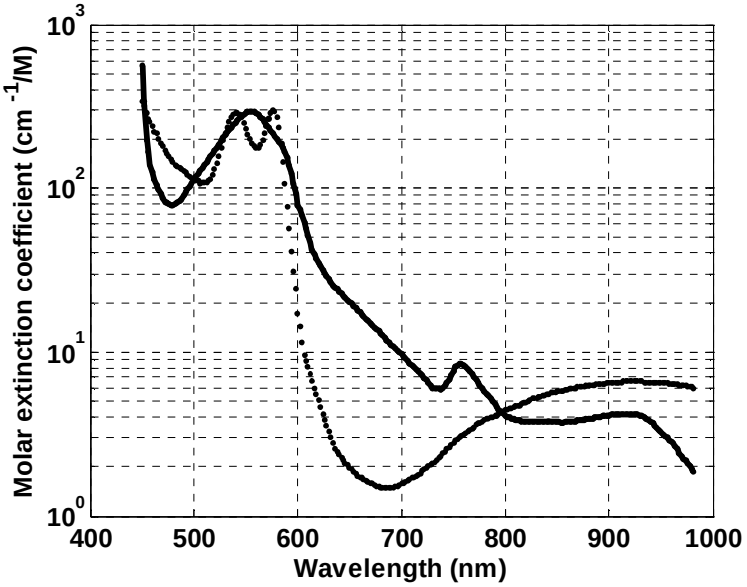

(a)

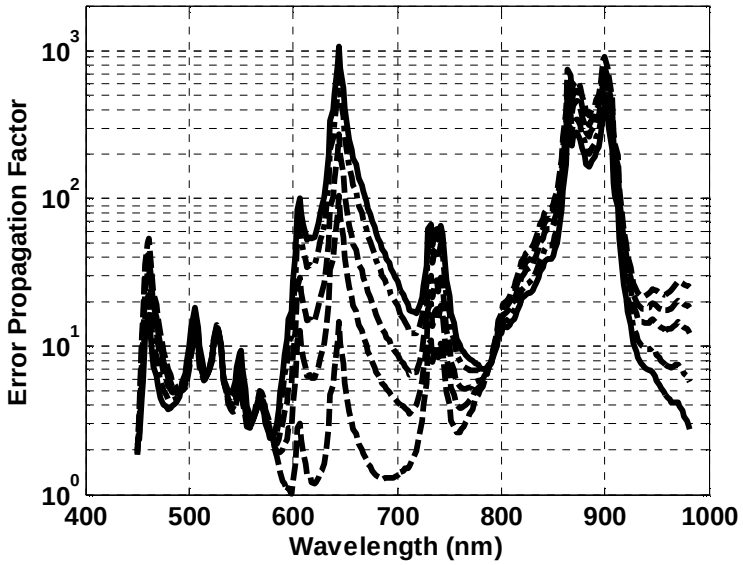

(b)

Fig. 5. Error propagation analysis. (a) Molar extinction spectra of oxygenated and deoxygenated hemoglobin (b) Error propagation factor (EPF) for inversion of SO_2 at different optical spectral bands. The solid lines show EPF at SO_2 values ranging from 100% (thick solid line) to 60% in 20% steps.

4. Optimal Choice of Ultrasonic Detection Parameters

Linearity of peak PA signal amplitude with optical absorption coefficient

One of the major concerns of SO2 inversion from PA measurements is linearity of PA magnitude with respect to absorption coefficient. Equation (4) is valid only for small light absorption when $\mu_a a << 1$, where 'a' is the vessel radius and μ_a is the optical absorption in blood. However, in the chosen spectral range and transducer frequency band, it is not true for majority of resolvable blood vessels. Correspondingly, prior to applying the method for in vivo measurements, the linearity of the PA signal amplitude dependence on μ_a for highly absorptive objects, $\mu_a a \geq 1$, must be experimentally demonstrated.

Fig 6(a) shows the peak amplitude of experimentally measured PA signals from tubes of 0.25 mm, 0.5 mm, and 1 mm diameter filled with ink (Lake Placid Blue, Private Reserve Ink) at various concentrations. Measurements were performed using a 5 MHz transducer. This represents scaled model of blood vessel typically imaged by PAM; all problem length parameters – light absorption length, ultrasonic wavelength and cylinder radius are ten times bigger than in typical situation in vivo. Fig 6(b) shows the peak amplitudes of the experimentally measured PA signals with 100 times averaging from a 0.25 mm diameter tube filled with ink samples of different concentrations covering the absorption range of whole blood in the visible spectrum. Measurements were acquired using a 50 MHz central frequency transducer; however, due to frequency dependent ultrasonic absorption in the tube material, the measured central frequency was near 25 MHz. The experimental data coincide with a linear fit up to $\mu_a a \approx 2$. There is a good

correspondence between the experimental and theoretical data calculated by convolving the experimentally measured transient response of the ultrasonic transducer with the time domain photoacoustic pressure for cylindrically symmetric problems[29] with instant heat deposition for homogeneous cylinders uniformly illuminated by omni-directional scattered light given by:

$$H(\hat{\mu}_a,\xi)=\frac{\mu_a}{\pi}\int_0^{\pi/2}\int_0^{\pi}\exp(\mu_a(\xi\cos\theta-\sqrt{1-(\xi\sin\theta)^2})/\sin\varphi)\cos\varphi d\theta d\varphi\,.$$

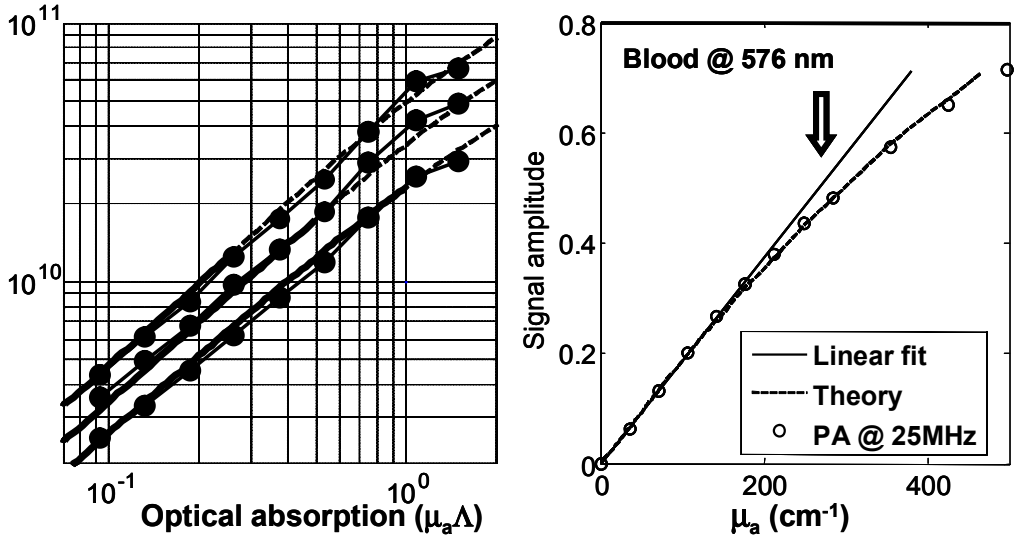

Fig. 6. Linearity of peak magnitude of photoacoustic pressure. The peak magnitude of the photoacoustic pressure (a) at a large distance from an uniformly illuminated cylinder as a function of the normalized optical absorption for normalized cylinder radii a=0.83 Λ (upper curve), a=0.625 Λ, and a=0.42Λ as compared to experimental data and (b) that from a 0.25 mm diameter cylinder tube versus the absorption coefficient for ink.

In vitro blood studies – comparison of SO_2 quantification using 25 and 10 MHz transducers

Validity of inversion scheme for SO_2 measurements was tested *in vitro* using anti-coagulated (citrate dextrose solution) bovine blood samples of different oxygenation levels. Two stock samples of fully oxygenated and deoxygenated blood were prepared by saturating the bovine blood with pure oxygen at 6^oC and carbon dioxide at 36^oC respectively. Four more samples of different oxygenation levels were prepared by mixing the two stock samples in predetermined volumetric ratios.[25] For comparison, NIRS measurements were made on hemolyzed (0.5% saponin, Sigma-Aldrich) blood samples using a spectrophotometer (GENESYS 20, Thermo Electron) in the wavelength range of 700-1000 nm with a step size of 4 nm.[26] The samples were then injected into tubes of 0.25-mm inner-diameter (TYGON S-54-HL, Norton Performance Plastics) and to prevent sedimentation, a steady flow of the blood sample through the tube was maintained by using a syringe pump (Barintree Scientific) at the rate of about 0.1 μl/s. Single point measurements were acquired using the PAM system at 12 wavelengths between 576 and 598 nm in steps of 2 nm. The SO_2 level of each sample was calculated from PAM measurements and the published spectra of Hb and HbO_2 using linear regression technique as discussed.

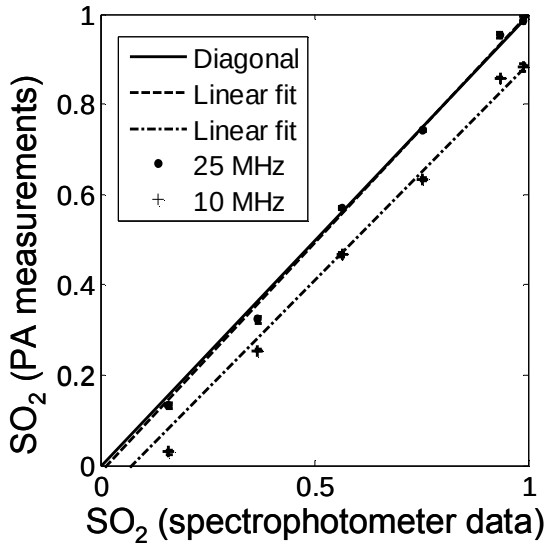

Fig. 7. Comparison of *in vitro* blood oxygenation measurements obtained with 25 and 10 MHz transducers. Inverted SO2 values from *in-vitro* photoacoustic measurements vs. that from optical measurements using chemically hemolyzed blood.

Fig 7 shows a plot of SO_2 measurements in whole bovine blood obtained using PAM against NIR spectrophotometric SO_2 measurements at different oxygenation levels using 25 MHz and 10 MHz transducers. With 25 MHz transducer, PA measurements agreed with spectrophotometric data with a systematic error (accuracy) of ~4%. With 10 MHz transducer, SO_2 data inverted from PA measurements gives large although systematic shift to lower values by about 10%. Variance in the PA measurements does not exceed 1%, which demonstrated the high sensitivity of PAM in measuring SO_2. Correspondingly, *in vitro* studies demonstrate high linearity of the PA peak amplitude

measurements with respect to μ_a and high accuracy and sensitivity of the PAM in quantitative measurement of SO_2 within its realm of application ($\mu_a \Lambda < 1$).

The effect of transducer focus on SO_2 measurements was found to be negligibly small. With 25 MHz transducer, the highest deviation of SO_2 measured at ±0.5 mm from transducer focus from the SO_2 value calculated at focus does not exceed 2%.

In vivo blood oxygenation measurements

The ultimate goal of PA measurements is to quantify blood oxygenation *in vivo*, which has been done on Sprague Dawley rats (~200 g, Charles River Breeding Laboratories). All experimental animal procedures were carried out in conformity with the guidelines of the United States National Institutes of Health (NIH 1985) [30]. The laboratory animal protocol for this work was approved by the ULAC of Texas A&M University.

Before imaging, hair was removed from the back of the rat using commercial hair remover lotion. Intramuscular injection of 87 mg/kg Ketamine plus 13 mg/kg Xylasine was administered to anesthetize the rat and the animal was kept motionless throughout the experiment with supplemental injections of similar anesthetic mixture (~50 mg/kg/hour). The area to be scanned was fixed using an in-house made holder and ultrasound coupling was provided by using water and ultrasound gel. The body temperature of the animal was maintained throughout the experiment. Spectral b-scan images were obtained at the four wavelengths of 578 nm, 584 nm, 590 nm, 596 nm. Without signal averaging, spectral images of a 10 mm × 3mm cross-section took about 1.5 minutes. The arterial blood saturation and heart rate of the animal was monitored

through out the experiment using a pulse oximeter (Nonin Medical, Inc). The animal recovered without noticeable health problems after the experiment.

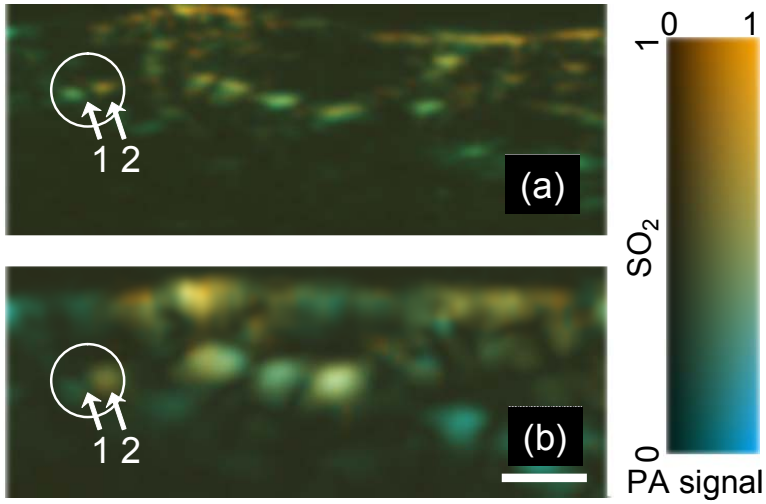

Fig. 8. *In vivo* B-scan (cross-sectional) image of rat skin vasculature. Using (a) 25 MHz and (b) 10 MHz ultrasonic transducers. Distribution of inverted SO_2 is color coded: pixel color represents SO_2 change from 0 (blue) to 100% (red); pixel intensity represents photoacoustic signal magnitude. SO_2 values for vein (1) and artery (2) are discussed in the article body. Bar size is 1mm, image is expanded two times vertically for clarity.

Peak positions of PA signal identified along each A-line at the isosbestic wavelength of 584 nm were used to get the corresponding spectral PA signal amplitudes and pixel by pixel calculation of SO_2 was done for each peak. Figs 8(a) and (b) show the

cross-sectional images of blood vessels obtained by employing 25 MHz and 10 MHz transducers respectively. The SO_2 values were visualized using pseudo color based on the SO_2 values. Blood provides endogenous contrast for PA signals and hence, the brightness of each pixel on the cross-sectional image reflects the total hemoglobin concentration in the corresponding voxel. Correspondingly, the image matrix of SO_2 values was multiplied with the "brightness" image to show both the SO_2 value and discern blood vessels from surrounding tissue based on total hemoglobin concentration (see color bar shown to the right of the image). Two well identifiable vessels were chosen for comparison of SO_2 values measured by 10 and 25 MHz transducers *in vivo*. Vessels marked 1 and 2 on the image showed SO_2 of 57% and 23% respectively using the 25 MHz transducer and 54% and 9% respectively with 10 MHz transducer. Although change of inverted SO_2 from PA data obtained with different central frequency transducers is consistent with theoretical predictions, it cannot explain significant underestimation of blood oxygenation which under normal conditions is expected to be about 98% for arterial blood and about 89% for venous blood.[31] This indicates the presence of some factors specific to *in vivo* measurements which influence SO_2 results. Most plausibly spectral dependent tissue (skin) optical absorption caused by blood in capillary network causes optical fluence on blood vessels to be spectral dependent and must be accounted for to make correct *in vivo* measurements.

5. Compensation for Spectral Dependence of Optical Fluence Reaching the Absorber

PA pressure generated is proportional to the product of local absorption coefficient and fluence distribution. From equations (4) used in this study, relating the amplitude of PA signal to the total absorption, it is evident that the fluence reaching the blood vessel is assumed to be a constant for all of the wavelengths used for spectral PA measurements. This constant factor is incorporated in the proportionality constant denoted by *K* in the equations. Although this assumption is valid for phantom studies and *in vitro* measurements, it does not hold for *in vivo* measurements. Wavelength dependence of light distribution within the tissue can significantly reduce the accuracy of derived parameters such as blood oxygenation level, if not accounted for. It is reasonable to state that the spectral dependence of laser fluence reaching the absorber would be largely be defined by the optical properties of biological tissue. It is surmised that the blood in the capillary network of the tissue imparts its spectral signature on the fluence reaching the blood vessel of interest. Subsequently, the optical properties μ_a and μ_s' of the tissue can be modeled based on the assumption stated. Beer's law of exponential decay holds for non-scattering medium, i.e. when $\mu_s = 0$. Considering that blood has very high absorption in the visible wavelength range, the condition of $\mu_a >> \mu_s'$ holds and hence exponential decay of fluence can be assumed. Hence, the decay constant would mainly depend on the absorption coefficient of blood in the capillary network. Other parameters that could affect the fluence reaching the absorber include tissue absorption, skin absorption etc.

The goal is to compensate for the spectral dependence of fluence reaching the blood vessel. There are well known methods such as Monte Carlo to simulate photon transport in tissue. For the problem at hand, modeling the illumination condition and blood vessel network in tissue, accounting for inter-subject variability is a challenge. Instead, a simplistic exponential decay model has been proposed for the fluence. If it is possible to experimentally measure the fluence from the PA signal by introducing a highly absorbing object with a flat spectrum would enable us to utilize the exponential decay model to estimate the fluence at a given depth. For this purpose, it is proposed that a small black film be introduced under the skin of the animal. Amplitude of spectral PA measurements performed on an area enclosing the black film would give us the fluence at the depth of the black insert, since the optical spectrum of such an object is flat. According to the model, $I = I_o \exp(-\mu_a z)$, where μ_a is the optical absorption coefficient and can be influenced by many parameters such as skin absorption, blood in the capillary network, tissue absorption etc and z is the distance of the black insert from the skin surface.

To measure skin optical attenuation, black polyethylene film was inserted under rat skin as shown in Fig 9(a). During the experiment, a Pulse Oximeter (8600 V, Nonin Medical, MN) was used to monitor the heart rate and arterial blood oxygenation which showed a value of 98%. PAM images were acquired at 15 wavelengths for 2mm x 2mm area enclosing the black insert. Spectra obtained from PA measurements shown on Fig 9(b) are average spectra for different scanning lines normalized on their own mean magnitude. Dashed line corresponds to the best fit assuming exponential decay of optical

fluence: $I = I_o \exp(-z \cdot [Hb].\varepsilon(\lambda, SO_2))$, $[Hb].\varepsilon(\lambda, SO_2)$ which gives the optical absorption coefficient and average SO_2 are unknown quantities. As it can be seen, PA signal amplitude varies significantly (up to ±30%) along surface of the insert. However, the optical wavelength dependence of PA signal amplitude shows the same trend. This relative stability of dermal spectral properties allows the following compensation technique. Owing to large difference in PA spectra of veins and arteries, one can easily identify them. Then measured PA spectra can be corrected for fluence change $I = I_o \exp(-z \cdot [Hb] \cdot \varepsilon(\lambda, SO_2))^{\alpha}$ where α is a factor introduced to accommodate the effects of other parameters such as tissue absorption. Since SO_2 in arteries changes very little, it is possible to find α by matching inverted arterial SO_2 with the pulse oximeter data and use it for fluence compensation of other vessels.

For the 25 MHz data shown in Fig. 8, upon compensation to obtain arterial SO_2 to be 86% (as was measured using pulse oximeter during experiment), the venous SO_2 value went up to 49% which seems physiologically more plausible as compared to 23% obtained without compensation.

Fig. 10 shows C-scan (maximum intensity projection) images of rat skin vasculature taken with a 50 MHz transducer. Each image was normalized on its maximum brightness value. Upon compensation, the resulting SO_2 measurements yield physiologically plausible result as it is shown in Fig. 11.

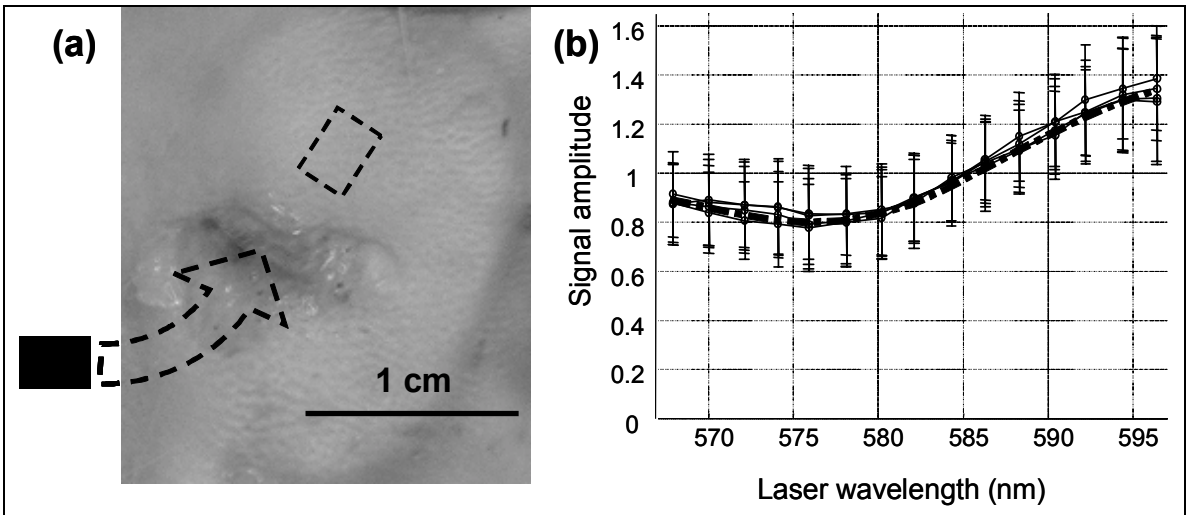

Fig. 9. Black insert study. (a) Insertion of 50 μm thick black polyethylene film under rat dermis and (b) the spectra of PA signals from the black insert taken *in vivo*.

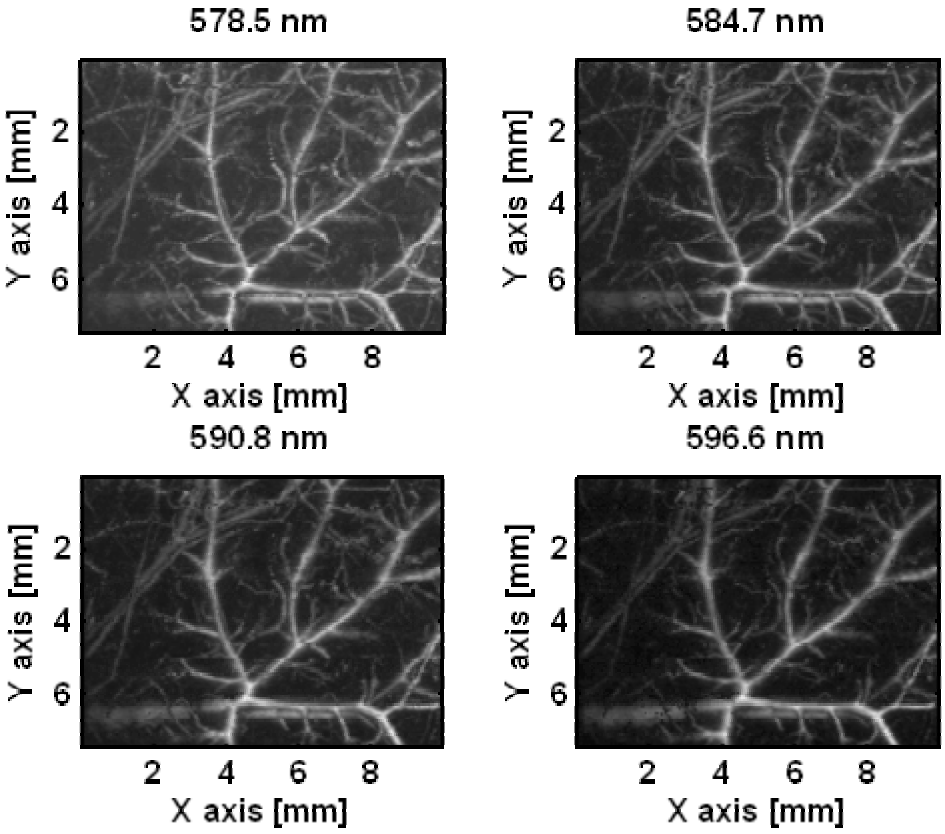

Fig. 10. C-scan (maximum intensity projection) images of rat skin vasculature taken with a 50 MHz transducer. Pixel brightness represents the PA intensity. Bar size is 1mm; each image was normalized on its maximum brightness value.

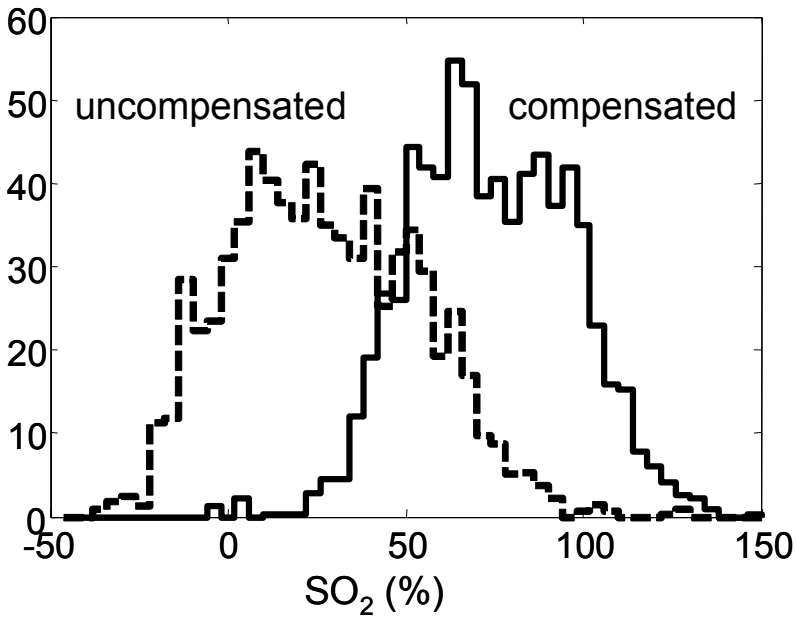

Fig. 11. Weighted distribution of SO_2 values for data from Fig. 10.

CHAPTER V

SUMMARY AND CONCLUSIONS

The aim of the project is to identify functional parameters that can be inverted from PAM measurements and to quantify the accuracy and sensitivity of the inversion procedure.

Phantom studies on ink mixtures and in vitro blood samples indicated the feasibility of extracting functional information from spectral PA measurements.

The stability of the inversion procedure was analyzed using propagation of error in measurements to error in inverted quantities. It was found that minimum inversion error occurs in the optical wavelength region of 570-600 nm and hence was chosen for the study. High blood absorption in this wavelength region also improves signal to noise ratio and also minimizes optical scattering.

To obtain ~4% accuracy in SO_2 measurements (independent of blood vessel size), the central frequency of ultrasonic transducer, 25 MHz for this wavelength region, should be high enough to satisfy the relation $\mu_a \Lambda < 1$. Results of i*n vitro* experiments on bovine blood samples of different oxygenation levels with 25 MHz and 10 MHz transducers were compared. The sensitivity was quantified to be ~1%.

To obtain accurate SO_2 values for *in vivo* measurements, one needs to account for spectral dependent optical attenuation. A method for compensation from data obtained using black insert study was proposed and tested and the improved results have been presented.

REFERENCES

1. L. Schallom and T. Ahrens, "Clinical application. Using oxygenation profiles to manage patients," Crit. Care. Nurs. Clin. North. Am. **11**, 437-446 (1999).

2. B. A. Teicher, J. S. Lazo, and A. C. Sartorelli, "Classification of antineoplastic agents by their selective toxicities toward oxygenated and hypoxic tumor cells," Cancer Res. **41**, 73-81 (1981).

3. R. H. Thomlinson and L. H. Gray, "The histological structure of some human lung cancers and the possible implications for radiotherapy." Br. J. Cancer **9**, 539-549 (1955).

4. R. A. Gatenby, H. B. Kessler, J. S. Rosenblum, L. R. Coia, P. J. Moldofsky, W. H. Hartz, and G. J. Broder, "Oxygen distribution in squamous cell carcinoma metastases and its relationship to outcome of radiation therapy," Int. J. Radiat. Oncol. Biol. Phys. **14**, 831-838 (1988).

5. M. Hockel, K. Schlenger, B. Aral, M. Mitze, U. Schaffer, and P. Vaupel, "Association between tumor hypoxia and malignant progression in advanced cancer of the uterine cervix. Cancer Res. **56**, 4509-4515 (1996).

6. X. Wang, Y. Pang, G. Ku, X. Xie, G. Stoica, and L. V. Wang, "Non-invasive laser-induced photoacoustic tomography for structural and functional imaging of the brain in vivo," Nat. Biotech. **21**, 803-6 (2003).

7. B. Venkatesh, R. Meacher, M. J. Muller, T. J. Morgan, and J. Fraser, "Monitoring tissue oxygenation during resuscitation of major burns," J. Trauma **50**, 485-94 (2001).

8. F. Gottrup, "Oxygen in wound healing and infection," World J. Surg. **28**, 312–315 (2004).

9. M. Henke, C. Bechtold, F. Momm, W. Dorr, R. Guttenberger, "Blood haemoglobin level may affect radiosensitivity—preliminary results on acutely reacting normal tissues," Int. J. Radiat. Oncol. Biol. Phys. **48**, 339-345 (2000).

10. J. D. Whitney, "Physiological effects of tissue oxygenation on wound healing," Heart and Lung **18**, 466-474 (1989).

11. M. Salman, G. K. Glantzounis, W. Yang, F. Myint, G. Hamilton, and A. M. Seifalian, "Measurement of critical lower limb tissue hypoxia by coupling chemical and optical techniques," Clin. Sci. **108**, 159-165 (2005).

12. S. Beckert, M. B. Witte, A. Königsrainer, and S. Coerper, "The impact of the micro-lightguide O2C for the quantification of tissue ischemia in diabetic foot ulcers," Diabetes Care, **27**, 2863–2867 (2004).

13. A. Torricelli, V. Quaresima, A. Pifferi, G. Biscotti, L. Spinelli, P. Taroni, M. Ferrari, and R. Cubeddu, "Mapping of calf muscle oxygenation and haemoglobin content during dynamic plantar flexion exercise by multi-channel time-resolved near infrared spectroscopy," Phys. Med. Biol. **49**, 685-699 (2004).

14. W. A. Wilmer, O. Voroshilova, I. Singh, D. F. Middendorf, and F. G. Cosio, "Transcutaneous oxygen tension in patients with calciphylaxis," American Journal of Kidney Diseases **37**, 797-806 (2001).

15. M. G. Sowa, J. R. Mansfield, G. B. Scarth, and H. H. Mantsch, "Noninvasive assessment of regional and temporal variations in tissue oxygenation by near-infrared spectroscopy and imaging," Applied Spectroscopy **51**, 143-152 (1997).

16. K. C. Young, R. Railton, A. D. B. Harrower, and R. W. Brookes, "Transcutaneous oxygen tension measurements as a method of assessing peripheral vascular disease," Clin. Phys. Physiol. Meas. **2**, 147-151 (1981).

17. J. A. Wahr, K. K. Tremper, S. Samra, and D. T. Delpy, "Near-infrared spectroscopy: theory and applications," J. Cardiothorac. Vasc. Anesth**. 10**, 406-418 (1996).

18. R. P. Mason, P. P. Antich, E. E. Babcock, A. Constantinescu, P. P. Peschke, and E. W. Hahn, "Non-invasive determination of tumor oxygen tension and local variation with growth," Int. J. Radiat. Oncol. Biol. Phys. **29**, 95-103 (1994).

19. V. Kamat, "Pulse oximetry," Indian J. Anaesth. **46**, 261-268 (2002).

20. J. P. Hornak, *Encyclopedia of imaging science and technology* (John Wiley & Sons, Inc.), New York, (2002).

21. M. C. Krishna, N. Devasahayam, J. A. Cook, S. Subramanian, P. Kuppusamy, and J. B. Mitchell, "Electron paramagnetic resonance for small animal imaging applications," ILAR Journal **42**, 209-218 (2001).

22. K. Maslov, G. Stoica, and L. V. Wang, "*In vivo* dark-field reflection-mode photoacoustic microscopy," Opt. Lett. **30**, 625-627 (2005).

23. K. Maslov, and L. V. Wang, "High-resolution photoacoustic vascular imaging in vivo using a large-aperture acoustic lens," Proc. SPIE **5697**, 7-14 (2005).

24. S. L. Jacques and S. A. Prahl, “Absorption spectra for biological tissues,” (Oregon Medical Laser Center, Portland, Oreg., 2004), http://omlc.ogi.edu/spectra/hemoglobin/index.html.

25. P. Scheid and M. Meyer, “Mixing technique for study of oxygen-hemoglobin equilibrium: a critical evaluation,” J. Appl. Physiol. **45**, 818-22 (1978).

26. M. U. Tsao, S. S. Sethna, C. H. Sloan, and L. J. Wyngarden, “Spectrophotometric determination of the oxygen saturation of whole blood,” J. Biol. Chem. **217,** 479-88 (1955).

27. C. L. Yapura, V. K. Kinra, and K. Maslov, "Measurement of six acoustical properties of a three-layered medium using resonant frequencies" J. Acoust. Soc. Am. **115**, 57-65 (2004).

28. J. Laufer, C. Elwell, D. Delpy, and P. Beard, “In vitro measurements of absolute blood oxygen saturation using pulsed near-infrared photoacoustic spectroscopy: accuracy and resolution,” Phys. Med. Biol. **50**, 4409–4428 (2005).

29. G. J. Diebold, T. Sun, and M. I. Khan, “Photoacoustic monopole radiation in one, two, and three dimensions,” Physical Review Letters, **69**, 3384-3387, (1991).

30. NIH guide for the care and use of laboratory animals (U.S. Government printing Office: Washington DC), (1985).

31. H. Kobayashi and N. Takizawa, “Oxygen saturation and pH changes in cremaster microvessels of the rat,” Am. J. Physiol. **270**, H1453-61, (1996).

VITA

Name	Mathangi Sivaramakrishnan
Educational Background	Bachelor of Engineering (Hons.), Electronics and Instrumentation Birla Institute of Technology and Science June 2001 Master of Science (Hons.), Biological Sciences Birla Institute of Technology and Science June 2001
Permanent address	131 Church Road, #9-D North Wales, PA 19454